

Real-time Control of a Magnetic Levitation System for Time-varying Reference Tracking

Eduardo Giraldo

Abstract—In this work, a design and implementation of a modified PID for tracking time-varying references are designed. The modified PID structure allows the reduction of the zeros added by the classical PID structure. The design of the controller is performed by considering time features such as settling time and maximum overshoot. The proposed controller is implemented and evaluated over a Hardware-in-the-Loop structure for real-time control performance. The controller is designed around an operational point and is evaluated for initial conditions, constant references, and time-varying references in terms of settling time and maximum overshoot. As a result, the modified PID structure shows advantages over the classical PID structure in terms of settling-time, maximum overshoot, and fidelity to the designed features.

Index Terms—Real-time, PID control, Magnetic Levitation, Time-varying reference.

I. INTRODUCTION

THE design of PID controllers over nonlinear systems is usually performed by using the transfer function $H(s)$ of the system computed by a linear approximation of the nonlinear system around an operational point [1]. Several controllers can also be applied over nonlinear systems, such as variable structure controllers [2], adaptive robust controllers [3] or intelligent controller [4]. It is worth noting that a key factor in the design of controllers over real systems is the evaluation of the controller over simulated and real prototypes [5]. These prototypes are usually build-up by using Hardware-In-the-Loop (HIL) strategies or Software-In-the-Loop (SIL) structures, being the HIL structure the most common implementation to evaluate the effectiveness of the controller [6].

The common equation for a PID controller is defined as

$$u(t) = K_p e(t) + K_i \int e(\tau) d\tau + K_d \frac{de}{dt} \quad (1)$$

being K_p , K_i and K_d , the controller parameters, and $e(t)$ the tracking error computed as

$$e(t) = r(t) - y(t) \quad (2)$$

being $r(t)$ the reference of desired output signal and $y(t)$ the output of the system to be controlled [7].

The transfer function of the error-based PID controller of (1), defined as $C(s)$ is obtained by applying the Laplace transform over (1) as:

$$C(s) = K_p + \frac{K_i}{s} + K_d s \quad (3)$$

Manuscript received March 1, 2021; revised July 27, 2021. This work was carried out under the funding of the Universidad Tecnológica de Pereira, Vicerrectoría de Investigación, Innovación y Extensión. Research project: 6-20-7 “Estimación Dinámica de estados en sistemas multivariados acoplados a gran escala”.

Eduardo Giraldo is a Full Professor at the Department of Electrical Engineering, Universidad Tecnológica de Pereira, Pereira, Colombia. Research group in Automatic Control. E-mail: egiraldo@utp.edu.co.

being $U(s) = C(s)E(s)$ and considering that the tracking error is computed by

$$E(s) = R(s) - Y(s) \quad (4)$$

where the linearized plant to be controlled $H(s)$ around an operational point is defined as:

$$Y(s) = H(s)U(s) \quad (5)$$

The resulting block diagram of the closed-loop system considering (3), (5) and (4) is presented in Fig. 1.

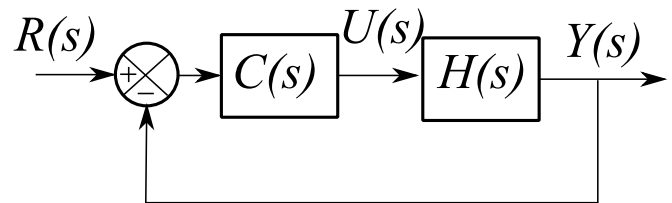


Fig. 1. Closed Loop controller

The success of the controller is highly dependant of the variability of the nonlinear function around the operational point where the system is operating [8]. The closed-loop transfer function can be obtained from the block diagram of Fig. 1, as follows:

$$Y(s) = H_{CL}R(s) \quad (6)$$

being H_{CL} defined as

$$H_{CL} = \frac{H(s)C(s)}{1 + H(s)C(s)} \quad (7)$$

Two design criteria are usually applied to design the controller [9]. The first one is based on the closed-loop characteristic equation $p_{LC}(s)$ which is the denominator of the closed-loop transfer function. This design criteria considers a desired equation for the closed-loop dynamics as $p_d(s)$ where the following relation is defined

$$p_{CL}(s) = p_d(s) \quad (8)$$

The second criteria considers the steady-state error e_{ss} by applying the Final Value Theorem computed as follows

$$e_{ss} = \lim_{t \rightarrow \infty} e(t) = \lim_{s \rightarrow 0} sE(s) \quad (9)$$

This design criteria considers that the absolute value of the steady-state error must achieve the following condition

$$|e_{ss}| \leq \epsilon \quad (10)$$

being $\epsilon > 0$ a threshold defined as the maximum permissible error for steady-state.

A methodology to design a PID controller for nonlinear systems around an operational point is presented in this

work. The methodology is obtained by combining (8) and (10) to design the controller, which results in a PID with time-varying tracking capabilities. A modified structure of the PID is used to reduce the effect of the zeros added by the controller structure. The proposed approach is validated by using a Magnetic Levitation nonlinear system around an operational point. The tracking capabilities are evaluated for initial conditions, constant references, and time-varying references. A HIL implementation of the Magnetic Levitation is used to evaluate the controller performance over a real system. This paper is organized as follows: section II describes the mathematical methods for modeling the magnetic levitation system and PID design. In section III the discrete equations used for real-time implementation of the controller and the HIL model of the magnetic levitation system are presented, and finally, in section IV the results and discussion are shown.

II. MATHEMATICAL MODEL

Consider the Magnetic Levitation model of Fig. 2 with current $u(t)$ as an input, and output $y(t)$ the displacement of mass M .

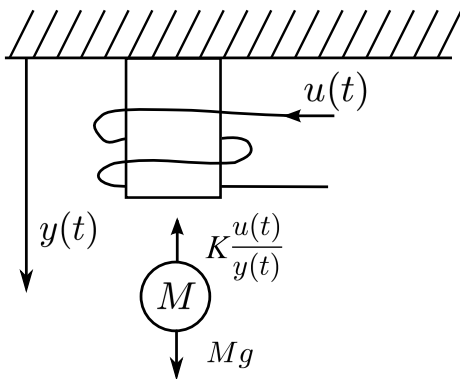


Fig. 2. Magnetic Levitation system

The system of Fig. 2 can be modeled by the following dynamical equation

$$Mg - K \frac{u(t)}{y(t)} = M\ddot{y} \quad (11)$$

By considering the operational point y_0 a constant, an equilibrium equation can be obtained

$$Mg - K \frac{u_0}{y_0} = 0 \quad (12)$$

where u_0 is obtained as

$$u_0 = \frac{Mgy_0}{K} \quad (13)$$

The linear approximation of (11) by using Taylor series approximation is obtained as

$$-\frac{Ky_0}{M} \Delta u(t) + \frac{Ku_0}{My_0^2} \Delta y(t) = \Delta \ddot{y} \quad (14)$$

By defining the parameters of the Magnetic Levitation system of (11) as $M = 0.05$, $K = 1$, $g = 9.8$ and $y_0 = 0.01$, the following linear equation is obtained:

$$-2000\Delta u(t) + 980\Delta y(t) = \Delta \ddot{y} \quad (15)$$

By applying the Laplace transform over (15) the transfer function of the Magnetic Levitation system of Fig. 2 is obtained

$$\Delta Y(s) = \frac{-2000}{s^2 - 980} \Delta U(s) \quad (16)$$

In Fig. 3, is presented the resulting linear closed-loop block diagram.

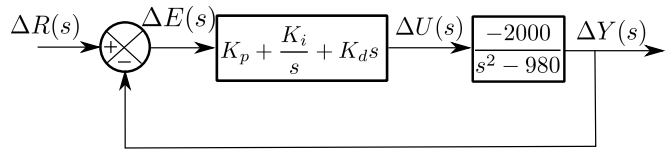


Fig. 3. Linear closed-loop block diagram

The steady-state error by using the Final Value theorem around an operational point is re-defined for the linear model as follows:

$$\Delta e_{ss} = \lim_{s \rightarrow 0} s \Delta E(s) \quad (17)$$

where $\Delta E(s)$ is obtained from the block diagram of Fig. 3 as follows:

$$\Delta E(s) = \frac{s^3 - 980s}{s^3 - 2000K_d s^2 - (2000K_p + 980)s - 2000K_i} \Delta R(s) \quad (18)$$

where the closed-loop characteristic equation $p_{CL}(s)$ is

$$p_{CL}(s) = s^3 - 2000K_d s^2 - (2000K_p + 980)s - 2000K_i \quad (19)$$

The first criteria for desired poles suggest that the dynamical behaviour of the closed-loop system must be determined by the following closed-loop complex poles:

$$s_{1,2} = -2 \pm j\sqrt{2}$$

However, since $p_{CL}(s)$ is a third order equation, an additional pole is required for the desired closed-loop equation $p_d(s)$. Therefore, the $p_d(s)$ is defined as

$$p_d(s) = (s + 2 + j\sqrt{2})(s + 2 - j\sqrt{2})(s + p) \quad (20)$$

being $s = -p$ with $p > 0$, the additional closed-loop pole. From (20), the $p_d(s)$ can be obtained as

$$p_d(s) = s^3 + (4 + p)s^2 + (4p + 6)s + 6p \quad (21)$$

By defining $p_d(s) = p_{CL}(s)$ the following relationships can be obtained

$$-2000K_i = 6p \quad (22)$$

$$-(2000K_p + 980) = 4p + 6 \quad (23)$$

$$-2000K_d = 4 + p \quad (24)$$

where is remarkable that, since $p > 0$ then K_i must be negative. It is noticeable the equations (22), (23) and (24) describe a system of three equations and four unknown quantities. In order to obtain an additional constraint and solve the system, the second criteria for steady-state error is used.

The second criteria considers the steady-state error of (17), where Δe_{ss} is equal to zero for $\Delta R(s)$ of type impulse and step. For time-varying references $\Delta R(s)$ of type ramp,

Δe_{ss} is not equal to zero. For this case, the steady-state error of (17) around and operational point is defined as

$$\Delta e_{ss} = \frac{980}{2000K_i} \quad (25)$$

where a $\Delta R(s) = \frac{1}{s^2}$ is used. By considering an $\epsilon = 0.05$ for the second criteria, the resulting constraint is

$$|\Delta e_{ss}| \leq 0.05 \quad (26)$$

and therefore

$$|K_i| \geq 98 \quad (27)$$

By choosing $K_i = -100$ the resulting p is $p = \frac{200000}{6}$ and therefore, K_p and K_d are

$$K_p = -67.15 \quad (28)$$

$$K_d = -16.66 \quad (29)$$

It is worth noting that the dominant response of the closed-loop system is approximated by the transfer function

$$Y(s) \approx \frac{\omega_n^2}{s^2 + 2\rho\omega_n s + \omega_n^2} R(s) \quad (30)$$

being the damping coefficient $\rho = 0.816$ and $\omega_n = 2.45$, which is presented in Fig. 4.

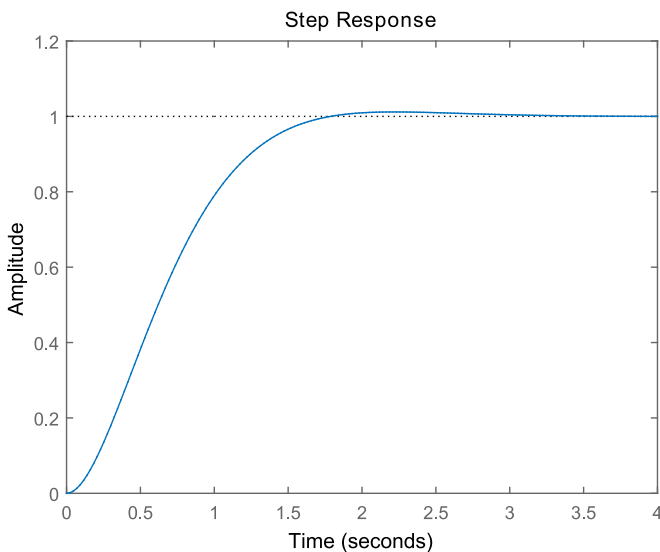


Fig. 4. Dominant response of the closed-loop system

It can be seen that the maximum overshoot is around 1.18% of the unitary step, and the settling time is around 2 seconds.

The resulting closed-loop transfer function is given by

$$\Delta Y(s) = \frac{-2000(K_d s^2 + K_p s + K_i)}{s^3 - 2000K_d s^2 - (2000K_p + 980)s - 2000K_i} \Delta R(s) \quad (31)$$

It is worth noting that the closed-loop transfer function has two zeros related directly to the controller, in comparison with the system that has no zeros. This phenomenon is due to the structure of the PID controller, where the derivative and proportional actions are related directly to the error. If the structure of Fig. 3 is modified as shown in Fig. 5 the resulting closed-loop has no zeros.

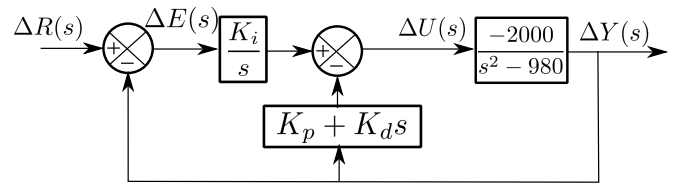


Fig. 5. Linear closed-loop with modified PID structure

By considering Fig. 5 the resulting closed-loop transfer function is now given by

$$\Delta Y(s) = \frac{-2000K_i}{s^3 - 2000K_d s^2 - (2000K_p + 980)s - 2000K_i} \Delta R(s) \quad (32)$$

where the closed-loop characteristic equation is hold, and where the transfer function for the error is now defined as

$$\Delta E(s) = \frac{s^3 - 2000K_d s^2 - (2000K_p + 980)s}{s^3 - 2000K_d s^2 - (2000K_p + 980)s - 2000K_i} \Delta R(s) \quad (33)$$

which has the same dynamics but for the selected values of the controller, the steady-state error for a ramp reference signal, is computed as

$$|\Delta e_{ss}| = 0.66 \quad (34)$$

Therefore, in order to reduce the steady-state error, and according to the stability criteria, the controller parameters must be recalculated. For time-varying references $\Delta R(s)$ of type ramp, Δe_{ss} is not equal to zero. For this case, the steady-state error of (17) around and operational point is defined as

$$\Delta e_{ss} = \frac{2000K_p + 980}{2000K_i} \quad (35)$$

where a $\Delta R(s) = \frac{1}{s^2}$ is used. By considering an $\epsilon = 0.05$ for the second criteria, the resulting constraint is

$$|\Delta e_{ss}| \leq 0.05 \quad (36)$$

III. REAL-TIME CONTROL EVALUATION

The real time implementation of the magnetic levitation system of (11) is performed by an approximation of the nonlinear model by using the backwards operator. The resulting nonlinear difference equation is defined as

$$y[k] = gh^2 - \frac{Kh^2 u[k-2]}{My[k-2]} + 2y[k-1] - y[k-2] \quad (37)$$

The discrete implementation of the PID controller in its classical or modified structure is based on the approximation by backward differences of derivative and integrative operators. The classical structure of the PID is implemented by using the following set of difference equations:

$$e_i[k] = e_i[k-1] + he[k] \quad (38)$$

$$e_d[k] = \frac{e[k] - e[k-1]}{h} \quad (39)$$

$$u[k] = K_p e[k] + K_d e_d[k] + K_i e_i[k] \quad (40)$$

being $e_i[k]$ the integral of the error $e[k]$ and $e_d[k]$ the derivative of the error $e[k]$, and h the sample time, where the error $e[k] = r[k] - y[k]$.

The block diagram of the Hardware-In-the-Loop (HIL) implementation of the classical PID controller over a Magnetic Levitation (MagLev) model is presented in Fig. 6.

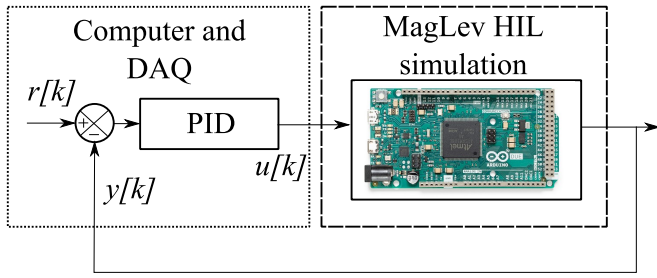


Fig. 6. Block diagram of the HIL implementation of the MagLev model for the classical PID controller

On the other hand, the modified structure of the PID is implemented by using the following set of difference equations:

$$e_i[k] = e_i[k - 1] + he[k] \quad (41)$$

$$y_d[k] = \frac{y[k] - y[k - 1]}{h} \quad (42)$$

$$u[k] = -K_p y[k] - K_d y_d[k] + K_i e_i[k] \quad (43)$$

being $y_d[k]$ the derivative of the output $y[k]$, $e_i[k]$ the integral of the error $e[k]$.

The block diagram of the HIL implementation of the modified PID controller over a MagLev model is presented in Fig. 7.

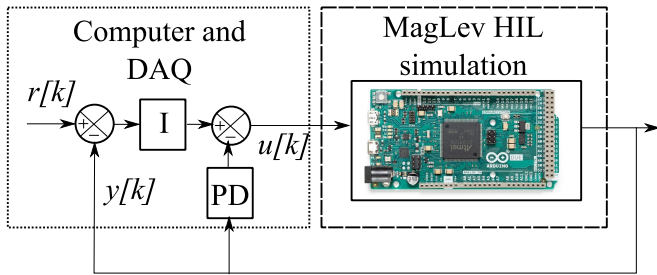


Fig. 7. Block diagram of the HIL implementation of the MagLev model for the modified PID controller

It is worth noting that the HIL implementation is performed over an ARDUINO DUE embedded system at 74MHz clock frequency, and the real-time controller is implemented in C++ by using a real-time clock with priority and a Data-Acquisition system USB-6009 from National Instruments with a sample time $h = 10$ milliseconds.

IV. RESULTS AND DISCUSSIONS

The designed control system is evaluated under unitary impulse, response, and ramp signals for the continuous closed-loop transfer functions to validate the design conditions. These reference signals are selected to validate the response of the closed-loop system to initial conditions, constant reference tracking, and time-varying reference tracking.

The response to a unitary impulse by using a classical PID structure is presented in Fig. 8.

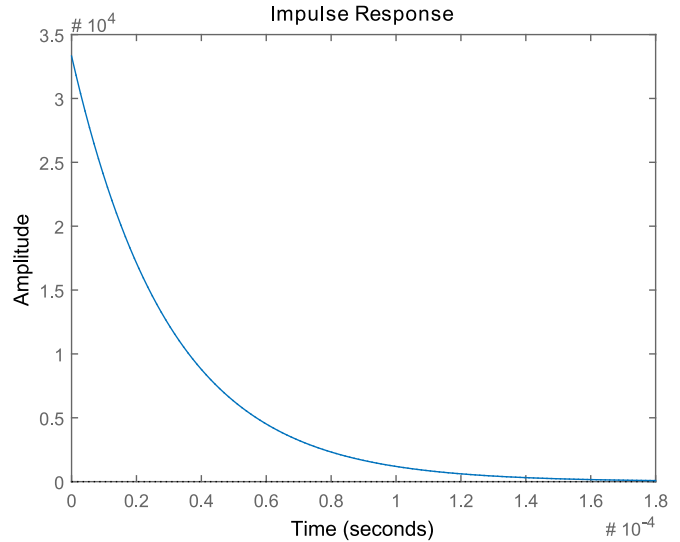


Fig. 8. Unitary impulse response by using a classical PID structure

The response to unitary step reference by using a classical PID structure is presented in Fig. 9.

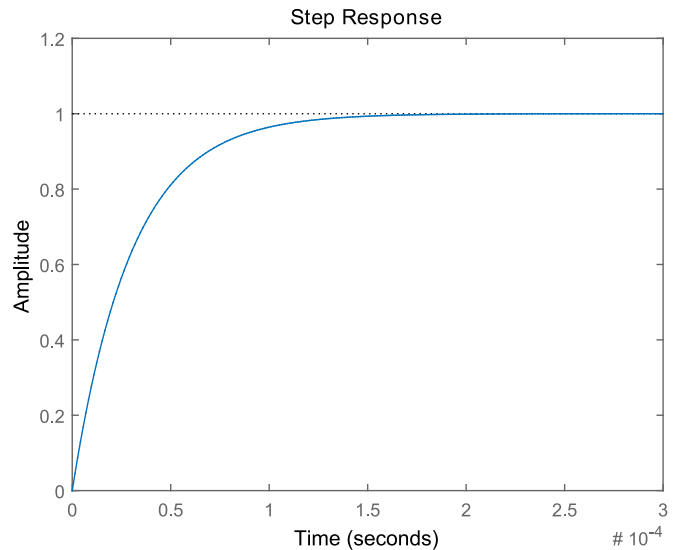


Fig. 9. Unitary step response by using a classical PID structure

It is noticeable that the tracking response of the closed-loop system obtained by using the classical PID structure, shown in Fig. 9, is not adequate since this response is not similar to the tracking response presented in Fig. 4 in terms of the settling-time. This effect is due to the zeros of the closed-loop system added by the PID classical structure.

The response to unitary ramp reference by using a classical PID structure is presented in Fig. 10.

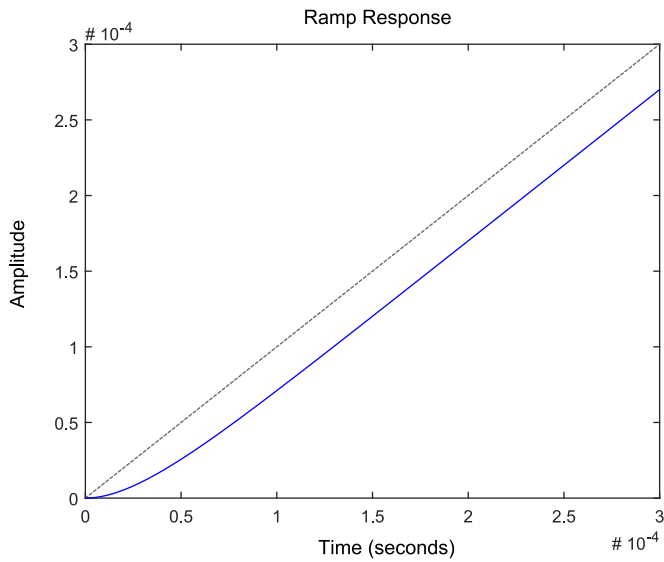


Fig. 10. Unitary ramp response by using a classical PID structure

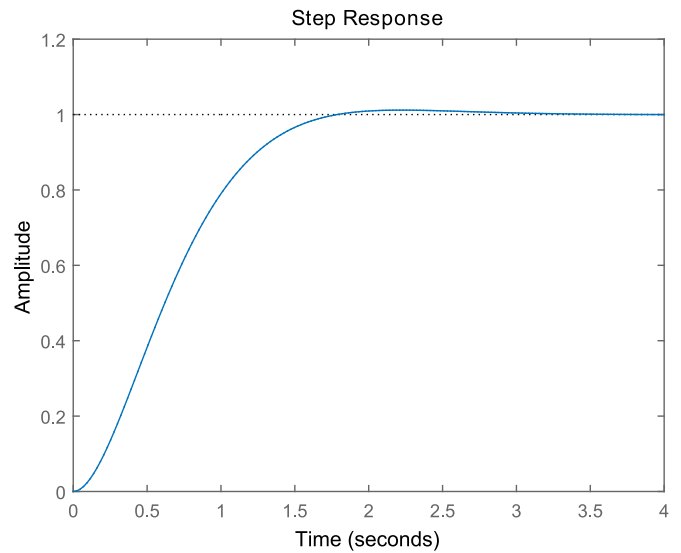


Fig. 12. Unitary step response by using a modified PID structure

The response to unitary ramp reference by using a modified PID structure is presented in Fig. 10.

The response to a unitary impulse by using a modified PID structure is presented in Fig. 11.

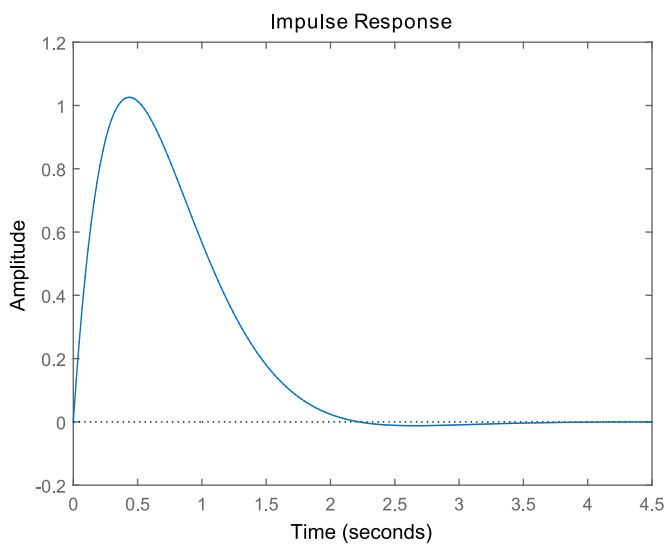


Fig. 11. Unitary impulse response by using a modified PID structure

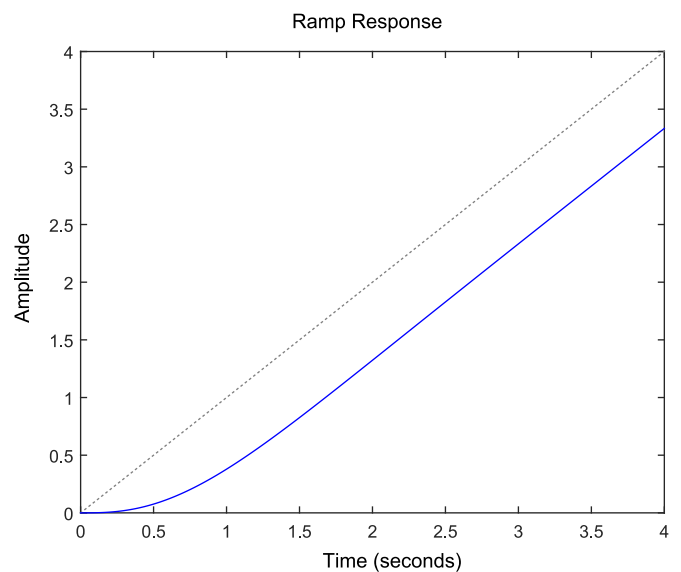


Fig. 13. Unitary ramp response by using a modified PID structure

It is noticeable that the tracking response of the closed-loop system obtained by using the modified PID structure, shown in Fig. 12, is quite similar to the tracking response presented in Fig. 4.

The response to unitary step reference by using a modified PID structure is presented in Fig. 9.

In Fig. 14 it is shown the real reference $r(t)$ and output $y(t)$ signals, considering a 5 seconds constant reference signal, by considering the modified PID structure. Two signals are presented by using the Digital-Analog -Converters of the micro-controller: $y(t)$ and $r(t)$. The signals are acquired by using an Uni-T, two channel, 100 MHz bandwidth, 1GS/s Oscilloscope.

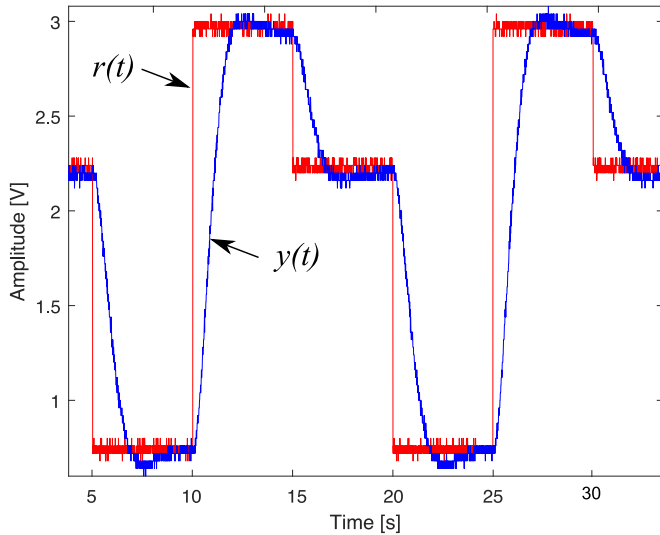


Fig. 14. Real-time 5 seconds constant reference tracking performance

It is worth noting that the output signal $y(t)$ in Fig. 14 tends to the reference $r(t)$ with zero steady-state error.

In Fig. 15 it is shown the real reference $r(t)$ and output $y(t)$ signals, considering a 4 seconds constant reference signal, by considering the modified PID structure.

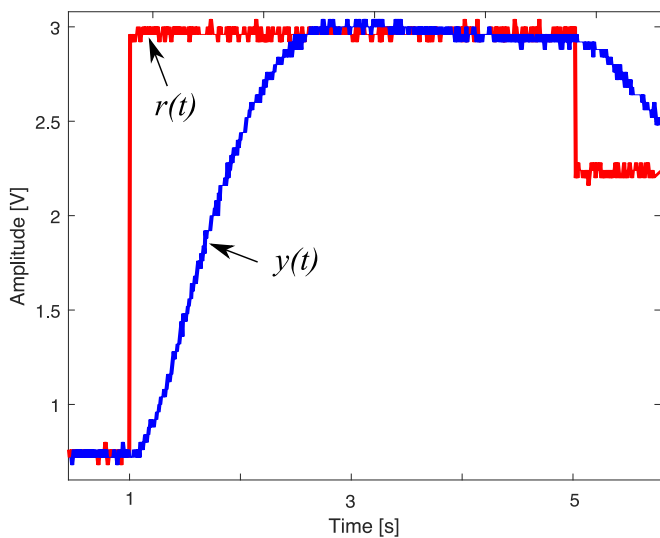


Fig. 15. Real-time 4 seconds constant reference tracking performance

In Fig. 16 it is shown the real reference $r(t)$ and output $y(t)$ signals, considering a 3 seconds time-varying reference signal. It can be seen that the output signal $y(t)$ tends to the reference $r(t)$ with a constant steady-state error, which is directly related to the slope of the reference.

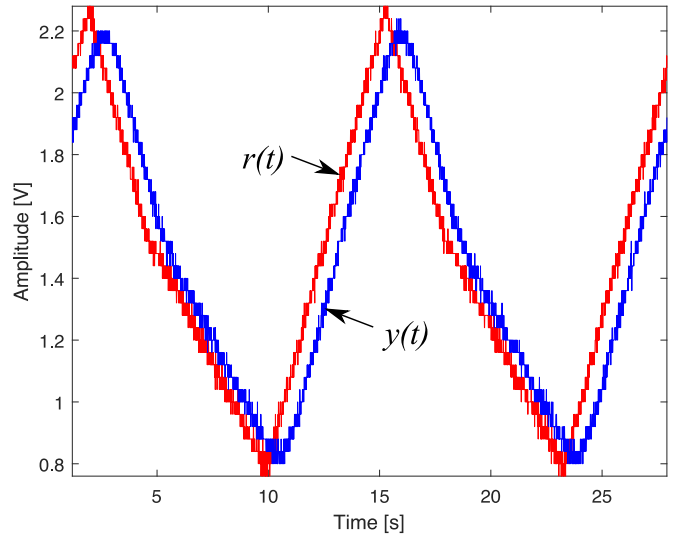


Fig. 16. Real-time time-varying reference tracking performance

In Fig. 17 it is shown the real reference $r(t)$ and output $y(t)$ signals, considering a 15 seconds time-varying reference signal, where is clear that $y(t)$ tends to the reference $r(t)$ with a constant steady-state error directly related to the change-rate of the reference.

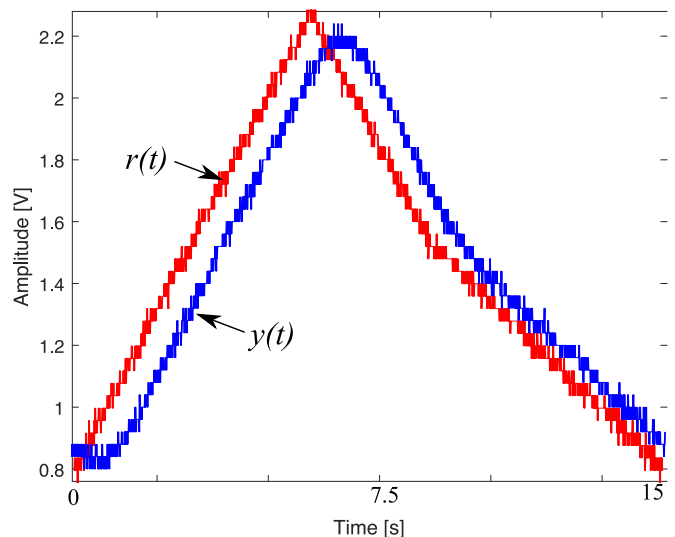


Fig. 17. Real-time time-varying reference tracking performance for 15 seconds segment

V. CONCLUSIONS

A methodology to design a PID controller for nonlinear systems around an operational point is presented in this work. The method is obtained by combining (8) and (10) to design the controller, which results in a PID with time-varying tracking capabilities. A modified structure of the PID is used to reduce the effect of the zeros added by the controller structure. As shown in the results, the proposed modified PID structure effectively reduces the impact of the zeros of the system compared to the classical PID structure. The Magnetic Levitation nonlinear system is implemented in a HIL structure with the real-time modified PID designed around an operational point. The tracking capabilities are evaluated for initial conditions, constant references, and time-varying references. The proposed approach increases

the performance of the classical control approach in terms of design fidelity for settling-time and maximum overshoot.

REFERENCES

- [1] K. J. Astrom and T. Haggglund, *Advanced PID control*. ISA, 2006.
- [2] F. Osorio-Arteaga, D. Giraldo-Buitrago, and E. Giraldo, "Sliding mode control applied to mimo systems," *Engineering Letters*, vol. 27, no. 4, pp. 802–806, 2019.
- [3] F. Osorio-Arteaga, J. J. Marulanda-Durango, and E. Giraldo, "Robust multivariable adaptive control of time-varying systems," *IAENG International Journal of Computer Science*, vol. 47, no. 4, pp. 605–612, 2020.
- [4] C. D. Molina-Machado and E. Giraldo, "Bio-inspired control based on a cerebellum model applied to a multivariable nonlinear system," *Engineering Letters*, vol. 28, no. 2, pp. 464–469, 2020.
- [5] T. Dohmke and H. Gollee, "Test-driven development of a pid controller," *IEEE Software*, vol. 24, no. 3, pp. 44–50, 2007.
- [6] A. Samiee, N. Tiefnig, J. P. Sahu, M. Wagner, A. Baumgartner, and L. Juhász, "Model-driven-engineering in education," in *2018 18th International Conference on Mechatronics - Mechatronika (ME)*, 2018, pp. 1–6.
- [7] D. E. Davidson and J. Chen, "Classical control revisited - re-examining the basics in the field," *IEEE Control Systems Magazine*, vol. 27, no. 1, pp. 20–21, 2007.
- [8] J. S. Velez-Ramirez, L. A. Rios-Norena, and E. Giraldo, "Buck converter current and voltage control by exact feedback linearization with integral action," *Engineering Letters*, vol. 29, no. 1, pp. 168–176, 2021.
- [9] F. Golnaraghi and B. C. Kuo, *Automatic Control Systems*, 9th ed. USA: Wiley, 2017.